2012

Benchmark Results for Testing Adaptive Finite Element Eigenvalue Procedures II (Cluster Robust Eigenvector and Eigenvalue Estimates)

Stefano Giani
Durham University

Luka Grubisic

Jeffrey S. Ovall
Portland State University, jovall@pdx.edu

BENCHMARK RESULTS FOR TESTING ADAPTIVE FINITE ELEMENT EIGENVALUE PROCEDURES II (CLUSTER ROBUST EIGENVECTOR AND EIGENVALUE ESTIMATES)

STEFANO GIANI, LUKA GRUBIŠIĆ, AND JEFFREY S. OVALL

Abstract. As a model benchmark problem for this study we consider a highly singular transmission type eigenvalue problem which we study in detail both analytically as well as numerically. In order to justify our claim of cluster robust and highly accurate approximation of a selected groups of eigenvalues and associated eigenfunctions, we give a new analysis of a class of direct residual eigenspace/vector approximation estimates Unlike in the first part of the paper, we now use conforming higher order finite elements, since the canonical choice of an appropriate norm to measure eigenvector approximation by discontinuous Galerkin methods is an open problem.

1. Introduction

Accurate computation of eigenvalues and eigenvectors of differential operators defined in planar regions has attracted considerable attention recently. A central paper in this body of work is the 2005 contribution of Trefethen and Betcke [10] on computing eigenpairs for the Laplacian on a variety of planar domains, by the method of particular solutions. This approach produced highly accurate eigenvalues—correct to 13 or 14 digits in some cases—but the approach is limited in its application scope to differential operators whose highest order coefficients are constant and lower order coefficients are analytic, see the discussion from [15]. In particular this means that handling anisotropic diffusion operators is excluded. For further discussion of recent research in this area see [9, 8, 30].

This limitation excludes many interesting eigenvalue model problems for composite materials, such as those which are of interest for methods of nondestructive sensing (cf. [1, 2]). Our interest in problems of this sort is motivated by considerations of photonic crystals and related problems, cf. [3, 16]. Although such problems are not directly addressed in this work, we do consider examples which have jump discontinuities in the coefficients of the highest and lowest order derivatives and therefore capture some of the computational difficulties which arise in photonic crystal applications. In [17], we used an *hp*-adaptive discontinuous Galerkin method, with duality-based (goal-oriented) adaptive refinement, to efficiently produce eigenvalue approximations having at least 10 correct digits for several model problems, including those with discontinuous coefficients.

Our experience thus far indicates that such *hp*-DG methods provide the most efficient means of computing eigenvalues in the discontinuous-coefficient case in terms of flops-per-correct-digit. However, the structure of DG-methods is such that only limited results are available on the accuracy of computed eigen*vector* approximations. This is, in part, due to the difficulty in choosing an appropriate norm for the analysis. The analytical framework that we have developed elsewhere for lower-order continuous elements ([7, 20]) uses native Hilbert space norms in an essential way, so standard DG norms appear very difficult to incorporate in this kind of analysis.

Motivated by this work on *h* adaptive finite element approximations we show a way to obtain reliable and efficient a-posteriori estimates in the *hp*-setting. As is standard for a-posteriori error analysis of eigenvalue problems, this task is reduced to analysis of associate boundary value problems. Our approach to this reduction from eigenvalue to boundary value problems is derived from operator-theoretic considerations, and very naturally leads to estimates of both eigenvalue and invariant subspace errors which are robust with respect to degenerate eigenvalues. The idea to reduce the study of the eigenvalue problem to the study of

Date: November 29, 2013.

2000 *Mathematics Subject Classification.* Primary: 65N30, Secondary: 65N25, 65N15.

Key words and phrases. eigenvalue problems, finite element methods, a posteriori error estimates, *hp*-apaptivity .

the associated boundary value problem is not new. However, the analysis from [7, 20] allows us to explicitly show that our bound are independent of the distances between clustered eigenvalues, but rather depend on the distance to the unwanted component of the spectrum. We obtain estimates which are both reliable as well as efficient. Furthermore, results from [7] indicate that the influence of the spectral separation is of higher order in the norm of the residual.

Because it is straight-forward to apply our framework in the analysis of approximations of eigenvectors of low regularity, $H^{1+\alpha}$ for some (small) $\alpha > 0$, as well as invariant subspaces corresponding to degenerate eigenvalues (those having multiplicity greater than one or clustered groups of eigenvalues), it seems useful to develop a continuous *hp*-adaptive scheme based on this approach. The aim is that a more robust theory might soon be complemented with computational efficiency which is competitive with its DG counterpart. The present work is a significant step in that direction.

For more information on *hp*-adaptive approximation methods for eigenvalue problems see [5, 24, 28]. These references mostly address a priori analysis of the eigenvalue/vector approximation problem. For a recent comprehensive treatment of a priori eigenvalue approximation error estimation see [13] and the references cited therein. For a recent account of a posteriori error analysis of *hp*-adaptive eigenvalue approximations see [4].

The rest of this paper is organized as follows. In Section 2 we introduce our model problem and basic notation related to its continuous and discrete versions, as well as some basic theory related to such eigenvalue problems. The notion of approximation defects and their relevance is discussed in Section 3, with results from [7, 20] extended for use in the present context. These extensions make possible the incorporation of results from [26, Section 3], which pertain to boundary value problem error estimation, to obtain efficient and reliable estimates of eigenvalue approximations, which is discussed in Section 4. Also in this section we present a subspace perturbation type result for the accuracy of eigenvectors—to assess the accuracy of the angle operator we use the Hilbert-Schmidt norm. In Section 4.2 we compare our results with other references in the literature. Section 5, which constitutes the bulk of the paper, is devoted to numerical experiments on a variety of different kinds of problems to assess the practical behavior of the proposed approach.

2. Model Problem and Discretization

Let $\Omega \subset \mathbb{R}^2$ be a bounded polygonal domain, possibly with re-entrant corners, and let $\partial\Omega_D \subset \partial\Omega$ have positive (1D) Lebesgue measure. We define the space $\mathcal{H} = \{v \in H^1(\Omega) : \ v_{|\partial\Omega_D} = 0\}$, where these boundary values are understood in the sense of trace. We are interested in the eigenvalue problem:

$$\text{Find } (\lambda, \psi) \in \mathbb{R} \times \mathcal{H} \text{ so that } B(\psi, v) = \lambda(\psi, v) \text{ and } \psi \neq 0 \text{ for all } v \in \mathcal{H} \ . \tag{1}$$

Here we have assumed

$$B(w, v) = \int_\Omega A\nabla w \cdot \nabla v + cwv \, dx, \tag{2}$$

and

$$(w, v) = \int_\Omega wv \, dx \tag{3}$$

is the standard L^2 inner-product. We will also assume that the diffusion matrix A is piecewise constant and uniformly positive definite a.e., the scalar c is also piecewise constant and non-negative. These assumptions are sufficient to guarantee that there are constants $\beta_0, \beta_1 > 0$ such that $B(v, w) \leq \beta_1 \|v\|_1 \|w\|_1$ and $B[v] \doteq B(v, v) \geq \beta_0 \|v\|_1^2$ for all $v, w \in \mathcal{H}$. In other words $B(\cdot, \cdot)$ is an inner product on $\mathcal{H}$, whose induced "energy"-norm $|\!|\!| \cdot |\!|\!|$ is equivalent to $\| \cdot \|_1$. The numbers β_0 and β_1 are referred to, respectively, as the coercivity and continuity constants for B.

Here and elsewhere, we use the following standard notation for norms and seminorms: for $k \in \mathbb{N}$ and $S \subset \Omega$ we denote the standard norms and semi-norms on the Hilbert spaces $H^k(S)$ by

$$\|v\|_{k,S}^2 = \sum_{|\alpha| \leq k} \|D^\alpha v\|_S^2 \qquad\qquad |v|_{k,S}^2 = \sum_{|\alpha| = k} \|D^\alpha v\|_S^2 \ , \tag{4}$$

where $\|\cdot\|_S$ denotes the L^2 norm on S. Additionally, we define $|\!|\!|\cdot|\!|\!|_S$ by

$$|\!|\!|v|\!|\!|_S^2 = \int_S A\nabla v \cdot \nabla v + cv^2\, dx\ , \tag{5}$$

recognizing that this may be a semi-norm. When $S = \Omega$ we omit it from the subscript. Our assumptions on A and c guarantee that there are local constants $\beta_{0S}, \gamma_{1S} > 0$ such that $\beta_{0S}|v|_{1,S}^2 \le |\!|\!|v|\!|\!|_S^2 \le \beta_{1S}\|v\|_{1,S}^2$, and the seminorm in the lower bound can be replaced with the full norm (after modifying β_{0S} if necessary) if $c(x) \ge c_S > 0$ on S.

2.1. **Notational conventions for eigenvalues and eigenvectors.** The variational eigenvalue problem (1)–(3) is attained by the positive sequence of eigenvalues

$$0 < \lambda_1 \le \lambda_2 \le \cdots \le \lambda_q \le \cdots \tag{6}$$

and the sequence of eigenvectors $(\psi_i)_{i\in\mathbb{N}}$ such that

$$B(\psi_i, v) = \lambda_i(\psi_i, v), \qquad \forall v \in \mathcal{H}, \qquad \text{and } (\psi_i, \psi_j) = \delta_{ij}\ . \tag{7}$$

Here we have counted the eigenvalues according to their multiplicity and we will also use the notation $\psi_i \perp \psi_j$ when $(\psi_i, \psi_j) = 0$ (when $i \ne j$). Furthermore, the sequence $(\lambda_i)_{i\in\mathbb{N}}$ has no finite accumulation point; and due to the Peron-Frobenius theorem we know that, in the case in which Ω is a path-wise connected domain, the inequality $\lambda_1 < \lambda_2$ holds and the eigenvector ψ_1 can be chosen so that ψ_1 is continuous and $\psi_1 > 0$ holds pointwise in Ω. We will also use the notation

$$\mathrm{Spec}_B := \{\lambda_i \ :\ i \in \mathbb{N}\}$$

to denote the spectrum of the variational eigenvalue problem (7) and we use

$$\mathfrak{M}(\lambda) := \mathrm{span}\{\psi \ :\ B(\psi, \phi) = \lambda(\psi, \phi), \quad \forall \phi \in \mathcal{H}\}$$

to denote the spectral subspace associated to $\lambda \in \mathrm{Spec}_B$. For variational eigenvalue problems like (7), which are defined by the form (2), the subspaces $\mathfrak{M}(\lambda)$, $\lambda \in \mathrm{Spec}_B$ are finite dimensional. Furthermore, let E_λ be the L^2 orthogonal projection onto $\mathfrak{M}(\lambda)$. Then

$$\sum_{\lambda\in\mathrm{Spec}_B} E_\lambda = I$$

and the spaces $\mathfrak{M}(\lambda) = \mathrm{Ran}\, E_\lambda$ and $\mathfrak{M}(\mu) = \mathrm{Ran}\, E_\mu$ are mutually orthogonal for $\lambda, \mu \in \mathrm{Spec}_B$ and $\lambda \ne \mu$.

Finally, note that

$$B(\psi, \phi) = \sum_{\lambda\in\mathrm{Spec(A)}} \lambda(\psi, E_\lambda \phi), \qquad \psi, \phi \in \mathcal{H}$$

and so we obtain an alternative representation of the energy norm

$$|\!|\!|\psi|\!|\!|^2 = B(\psi, \psi) = \sum_{\lambda\in\mathrm{Spec(A)}} \lambda(\psi, E_\lambda \psi), \quad \psi \in \mathcal{H}. \tag{8}$$

2.2. **Discrete eigenvalue/eigenvector approximations.** We discretize (1) using *hp*-finite element spaces, which we now briefly describe. Let $\mathcal{T} = \mathcal{T}_h$ be a triangulation of Ω with the piecewise-constant mesh function $h : \mathcal{T}_h \to (0, 1)$, $h(K) = \mathrm{diam}(K)$ for $K \in \mathcal{T}_h$. Throughout we implicitly assume that the mesh is aligned with all discontinuities of the data A and c, as well as any locations where the (homogeneous) boundary conditions change between Dirichlet and Neumann. Given a piecewise-constant distribution of polynomial degrees, $p : \mathcal{T}_h \to \mathbb{N}$, we define the space

$$V = V_h^p = \{v \in \mathcal{H} \cap C(\overline{\Omega}) :\ v\big|_K \in \mathbb{P}_{p(K)} \text{ for each } K \in \mathcal{T}_h\}\ ,$$

where $\mathbb{P}_j$ is the collection of polynomials of total degree no greater than j on a given set. Suppressing the mesh parameter h for convenience, we also define the set of edges $\mathcal{E}$ in $\mathcal{T}$, and distinguish interior edges $\mathcal{E}_I$, and edges on the Neumann boundary $\mathcal{E}_N$ (if there are any). Additionally, we let $\mathcal{T}(e)$ denote the one or two triangles having $e \in \mathcal{E}$ as an edge, and we extend p to $\mathcal{E}$ by $p(e) = \max_{K\in\mathcal{T}(e)} p(K)$. As is standard, we assume that the family of spaces satisfy the following regularity properties on $\mathcal{T}_h$ and p: There is a constant $\gamma > 0$ for which

(C1) $\gamma^{-1}[h(K)]^2 \le \mathrm{area}(K)$ for $K \in \mathcal{T}$,

(C2) $\gamma^{-1}(p(K)+1) \le p(K')+1 \le \gamma(p(K)+1)$ for adjacent $K, K' \in \mathcal{T}$, $\overline{K} \cap \overline{K'} \neq \emptyset$.

It is really just a matter of notational convenience that a single constant γ is used for all of these upper and lower bounds. The shape regularity assumption (C1) implies that the diameters of adjacent elements are comparable.

In what follows we consider the discrete versions of (1):

$$\text{Find } (\hat{\lambda}, \hat{\psi}) \in \mathbb{R} \times V \text{ such that } B(\hat{\psi}, v) = \hat{\lambda}(\hat{\psi}, v) \text{ for all } v \in V \ . \tag{9}$$

We also assume, without further comment, that the solutions are ordered and indexed as in (6), with $(\hat{\psi}_i, \hat{\psi}_j) = \delta_{ij}$. We are interested in assessing approximation errors in collections of computed eigenvalues and associated invariant subspaces. Let $s_m = \{\mu_k\}_{k=1}^m \subset (a,b)$ be the set of all eigenvalues of B, counting multiplicities, in the interval (a,b), and let $S_m = \operatorname{span}\{\phi_k\}_{k=1}^m$ be the associated invariant subspace, with $(\phi_i, \phi_j) = \delta_{ij}$. The discrete problem (9) is used to compute corresponding approximations $\hat{s}_m = \{\hat{\mu}_k\}_{k=1}^m$ and $\hat{S}_m = \operatorname{span}\{\hat{\phi}_k\}_{k=1}^m$, with $(\hat{\phi}_i, \hat{\phi}_j) = \delta_{ij}$.

Remark 2.1. When s_m consists of the smallest m eigenvalues, we use the absolute labelling $s_m = \{\lambda_k\}_{k=1}^m$ and $S_m = \operatorname{span}\{\psi_k\}_{k=1}^m$ instead of the relative labelling involving (μ_k, ϕ_k); and the analogous statement holds for the discrete approximations $\hat{s}_m$ and $\hat{S}_m$. This distinction is used in some of our results, such as Theorems 3.1 and 3.3.

3. Approximation Defects

3.1. **Approximation defects.** Let the finite element space $V \subset \mathcal{H}$ be given and let $\hat{s}_m$ and $\hat{S}_m$ be the approximations which are computed from V. We define the corresponding *approximation defects* as:

$$\eta_i^2(\hat{S}_m) = \max_{\substack{\mathcal{S} \subset \hat{S}_m \\ \dim \mathcal{S} = m-i+1}} \min_{\substack{f \in \mathcal{S} \\ f \neq 0}} \frac{|||u(f) - \hat{u}(f)|||^2}{|||u(f)|||^2} \ , \tag{10}$$

where $u(f)$ and $\hat{u}(f)$ satisfy the boundary value problems:

$$B(u(f), v) = (f, v) \text{ for every } v \in \mathcal{H} \tag{11}$$

$$B(\hat{u}(f), v) = (f, v) \text{ for every } v \in V \ . \tag{12}$$

In Theorems 3.1 and 3.3 below, we state key theorems from [20, 7], which show that these approximation defects would yield ideal error estimates for eigenvalue and eigenvector computation **if they could be computed**. This motivates the use of *a posteriori* error estimation techniques for boundary value problems to efficiently and reliably estimate approximation defects. In [20, 7], we used hierarchical bases to estimate the approximation defects when V was the space of continuous, piecewise affine functions. In Section 4 we show how to utilize the theory of residual based estimates for *hp*-finite elements from [26] in a similar fashion.

The following result concerns approximations $\hat{s}_{\mathrm{M}}$ and $\hat{S}_{\mathrm{M}}$ of the (complete) lower part of the spectrum. This is the reason why we have capitalized the dimension parameter $\mathrm{M} \in \mathbb{N}$, which is associated to the cluster of lowermost eigenvalues, as opposed to a given cluster of eigenvalues contained in the interval $\big(a,b\big)$.

Theorem 3.1. *Assume that $\lambda_{\mathrm{M}} < \lambda_{\mathrm{M}+1}$, and let $\hat{S}_{\mathrm{M}}$ be the span of first $\mathrm{M} \in \mathbb{N}$ eigenvectors of (9). If $\hat{S}_{\mathrm{M}} = \operatorname{span}\{\hat{\psi}_1, \cdots, \hat{\psi}_{\mathrm{M}}\}$ is such that $\frac{\eta_{\mathrm{M}}(\hat{S}_{\mathrm{M}})}{1-\eta_{\mathrm{M}}(\hat{S}_{\mathrm{M}})} < \frac{\lambda_{\mathrm{M}+1}-\hat{\lambda}_{\mathrm{M}}}{\lambda_{\mathrm{M}+1}+\hat{\lambda}_{\mathrm{M}}}$ then*

$$\frac{\hat{\lambda}_1}{2\hat{\lambda}_{\mathrm{M}}} \sum_{i=1}^{\mathrm{M}} \eta_i^2(\hat{S}_{\mathrm{M}}) \le \sum_{i=1}^{\mathrm{M}} \frac{\hat{\lambda}_i - \lambda_i}{\hat{\lambda}_i} \le C_{\mathrm{M}} \sum_{i=1}^{\mathrm{M}} \eta_i^2(\hat{S}_{\mathrm{M}}). \tag{13}$$

The constant C_M depends solely on the relative distance to the unwanted component of the spectrum (e.g. $\frac{\lambda_{\mathrm{M}}-\lambda_{\mathrm{M}+1}}{\lambda_{\mathrm{M}}+\lambda_{\mathrm{M}+1}}$).

The constant C_{M} is given by an explicit formula which is a reasonable practical overestimate, see [20, 7] for details. A similar result holds for the eigenvectors. We point the interested reader to [20, Theorem 4.1 and equation (3.10)] and [7, Theorem 3.10].

Remark 3.2. Although $\lambda_1 < \lambda_2$ for the particular problems we consider numerically in the present work, much of the theory carries over to problems where Ω is not pathwise connected, or the boundary conditions are periodic (as examples). In these cases the Peron-Frobenius theorem does not apply, and it is quite possible that the smallest eigenvalue is degenerate. If this is the case, and $\lambda_1 = \lambda_{\text{M}}$, then the constant $\hat{\lambda}_1/2\hat{\lambda}_{\text{M}}$ in (13) can be replaced by 1.

An important feature of these ideal estimates is that they are asymptotically exact, both as eigenvector as well as as eigenvalue estimators, as the following theorem indicates in the case of a single degenerate eigenvalue and its corresponding invariant subspace.

Theorem 3.3. *Let λ_q be a degenerate eigenvalue of multiplicty m, $\lambda_{q-1} < \lambda_q = \lambda_{q+m-1} < \lambda_{q+m}$. Let $\hat{S}_m = \hat{S}_m(\mathcal{T}) = \text{span}(\hat{\phi}_k) \subset V = V(\mathcal{T})$ be the computed approximation of the invariant subspace corresponding to λ_q. Then, taking the pairing of eigenvectors ϕ_i and Ritz vectors $\hat{\phi}_i$ as in* [20]*, we have*

$$\lim_{h\to 0} \frac{\sum_{i=1}^m \frac{|\hat{\mu}_i - \lambda_q|}{\hat{\mu}_i}}{\sum_{i=1}^m \eta_i^2(\hat{S}_m)} = 1 \quad , \quad \lim_{h\to 0} \frac{\sum_{i=1}^m \frac{B[\hat{\phi}_i - \phi_i]}{B[\phi_i]}}{\sum_{i=1}^m \eta_i^2(\hat{S}_m)} = 1 \ . \tag{14}$$

3.2. **A relationship with the residual estimates for a Ritz vector basis.** This section addresses the issue of the computability of $\eta_i(\hat{S}_m)$ by relating these quantities to the standard dual energy norm estimates of the residuals associated to the Ritz vector basis of $\hat{S}_m$.

In our notation the energy norm was denoted by $\|\!| \cdot |\!\|$ and we use $u(\cdot)$ and $\hat{u}(\cdot)$ to denote the solution operators from (11) and (12). We assume $\hat{\phi}_1, \ldots, \hat{\phi}_m$ are the Ritz vectors from $\hat{S}_m$, then for $i, j = 1, \ldots, m$, we define the matrices

$$E_{ij} = B\big(u(\hat{\phi}_i) - \hat{u}(\hat{\phi}_i), u(\hat{\phi}_j) - \hat{u}(\hat{\phi}_j)\big) \tag{15}$$

$$G_{ij} = B\big(u(\hat{\phi}_i), u(\hat{\phi}_j)\big). \tag{16}$$

These matrices were introduced in [20] under the name of the error and the gradient matrix. It was shown in [20] that $\eta_i(\hat{S}_m) = \lambda_i(E, G)$, where $\lambda_1(E, G) \le \cdots \le \lambda_m(E, G)$ are the eigenvalues of the generalized eigenproblem for the matrix pair (E, G). Furthermore, since G is a positive definite matrix it also holds that $\eta_i(\hat{S}_m) = \lambda_i(E, G) = \lambda_i(G^{-1/2}EG^{-1/2})$, where $\lambda_1(G^{-1/2}EG^{-1/2}) \le \cdots \le \lambda_m(G^{-1/2}EG^{-1/2})$ are the eigenvalues of the matrix $G^{-1/2}EG^{-1/2}$.

We further assume that $\hat{\phi}_i$, $i = 1, \cdots, m$ are among the Ritz vectors from the finite element subspace V, $V \supset \hat{S}_m$ from (12). The identity (15) implies that E is a Gram matrix for the set of vectors $u(\hat{\phi}_i) - \hat{u}(\hat{\phi}_i)$, $i = 1, \ldots, m$. If we assume that $\hat{S}_m$ does not contain any eigenvectors, then we conclude that E must be positive definite matrix. Furthermore, it always holds

$$\begin{aligned} \eta_i^2(\hat{S}_m) &= \lambda_i(G^{-1/2}EG^{-1/2}) \\ E_{ii} &= \mu_i^{-2}\|\!| u(\hat{\mu}_i\hat{\phi}_i) - \hat{u}(\hat{\mu}_i\hat{\phi}_i) |\!\|^2, \quad i = 1, \ldots, m \\ D_\mu &\le G \le (1 + \mathfrak{D}_l) D_\mu, \end{aligned} \tag{17}$$

where $D_\mu = \text{diag}(\hat{\mu}_1^{-1}, \ldots, \hat{\mu}_m^{-1})$ and $\mathfrak{D}_l = \|D_\mu^{-1/2}(G - D_\mu)D_\mu^{-1/2}\|$. Let us note that $\mathfrak{D}_l$ is a relative estimate, so it is expected that even for very crude finite element spaces V we have $\mathfrak{D}_l < 1$.

We now compute

$$\sum_{i=1}^m \lambda_i(D_\mu^{-1/2}ED_\mu^{-1/2}) = \text{trace}(D_\mu^{-1/2}ED_\mu^{-1/2}) = \sum_{i=1}^m E_{ii}\hat{\mu}_i,$$

and so conclude that

$$\frac{1}{1 + \mathfrak{D}_l} \sum_{i=1}^m E_{ii}\hat{\mu}_i \le \sum_{i=1}^m \eta_i^2(\hat{S}_m) \le \sum_{i=1}^m E_{ii}\hat{\mu}_i \ . \tag{18}$$

We summarize these considerations — using the identity (17) — in the following lemma.

Lemma 3.4. *It holds that*

$$\frac{1}{1+\mathfrak{D}_l}\sum_{i=1}^{m}\hat{\mu}_i^{-1}|||u(\hat{\mu}_i\hat{\phi}_i)-\hat{u}(\hat{\mu}_i\hat{\phi}_i)|||^2 \le \sum_{i=1}^{m}\eta_i^2(\hat{S}_m) \le \sum_{i=1}^{m}\hat{\mu}_i^{-1}|||u(\hat{\mu}_i\hat{\phi}_i)-\hat{u}(\hat{\mu}_i\hat{\phi}_i)|||^2 \ . \tag{19}$$

4. *hp*-Error Estimation and Adaptivity in the Eigenvalue Context

Using Lemma 3.4, we have reduced the problem of estimating the approximation defects, and hence the error in our eigenvalue/eigenvector computations, to that of estimating error in associated boundary value problems. In particular, we must estimate $|||u(\hat{\mu}_i\hat{\phi}_i)-\hat{u}(\hat{\mu}_i\hat{\phi}_i)|||^2$ for each Ritz vector, where $\hat{S}_m = \mathrm{span}\{\hat{\phi}_1,\ldots,\hat{\phi}_m\}$ is our approximation of $S_m = \mathrm{span}\{\phi_1,\ldots,\phi_m\}$. We modify key results from [26], which were stated only for the Laplacian, to our context. The identity $\hat{u}(\hat{\mu}_i\hat{\phi}_i)=\hat{\phi}_i$, makes our job easier. We define the element residuals R_i for $K\in\mathcal{T}$, and the edge (jump) residuals r_i for $e\in\mathcal{E}$, by

$$R_i|_K = \hat{\mu}_i\hat{\phi}_i - c\hat{\phi}_i + \nabla\cdot A\nabla\hat{\phi}_i \ , \tag{20}$$

$$r_{i|_e} = \begin{cases} -(A\nabla\hat{\phi}_i)_{|_K}\cdot\mathbf{n}_K - (A\nabla\hat{\phi}_i)_{|_{K'}}\cdot\mathbf{n}_{K'} & , e\in\mathcal{E}_I \\ -(A\nabla\hat{\phi}_i)_{|_K}\cdot\mathbf{n}_K & , e\in\mathcal{E}_N \end{cases} . \tag{21}$$

For interior edges $e\in\mathcal{E}_I$, K and K' are the two adjacent elements, having outward unit normals $\mathbf{n}_K$ and $\mathbf{n}_{K'}$, respectively; and for Neumann boundary edges $e\in\mathcal{E}_N$ (if there are any), K is the single adjacent element, having outward unit normal $\mathbf{n}_K$. We note that R is a polynomial of degree no greater than $p(K)$ on K, and r is a polynomial of degree no greater than $p(e)$ on e.

Our estimate of $\varepsilon_i^2 = \sum_{K\in\mathcal{T}}\varepsilon_i^2(K) \approx |||u(\hat{\mu}_i\hat{\phi}_i)-\hat{u}(\hat{\mu}_i\hat{\phi}_i)|||^2$ is computed from local quantities,

$$\varepsilon_i^2(K) = \left(\frac{h(K)}{p(K)}\right)^2\|R_i\|_{0,K}^2 + \frac{1}{2}\sum_{e\in\mathcal{E}_I(K)}\frac{h(e)}{p(e)}\|r_i\|_{0,e}^2 + \sum_{e\in\mathcal{E}_N(K)}\frac{h(e)}{p(e)}\|r_i\|_{0,e}^2 \ , \tag{22}$$

where $\mathcal{E}_I(K)$ and $\mathcal{E}_N(K)$ denote the interior edges and Neumann boundary edges of K, respectively. An inspection the proof of [26, Lemma 3.1] (which was stated for the Laplacian) makes the following assertion clear.

Lemma 4.1. *There is a constant $C>0$ depending only on the hp-constant γ and the coercivity constant β_0, such that $|||u(\hat{\mu}_i\hat{\phi}_i)-\hat{u}(\hat{\mu}_i\hat{\phi}_i)|||^2 \le C\varepsilon_i^2$.*

A few remarks are in order concerning the lemma above and how it relates to [26, Lemma 3.1]. First, the bound in [26, Lemma 3.1] includes an additional term involving the difference between the righthand side (in our case ϕ_i) and its projection on K into a space of polynomials. This additional term only arises in their result because they have chosen to use the projection of the righthand side, instead of the righthand side itself, to define the element residual (here called R_i). They do this in order to employ certain polynomial inverse estimates, which hold in our case outright because our righthand sides are piecewise polynomial. Their result also involves a parameter $\alpha\in[0,1]$, which we have taken to be 0. The result [26, Lemma 3.1] is based on Scott-Zhang type quasi-interpolation, which naturally gives rise to errors measured in H^1. Mimicking their arguments with our indicator, one would arrive at a result of the form

$$|||u(\hat{\mu}_i\hat{\phi}_i)-\hat{u}(\hat{\mu}_i\hat{\phi}_i)||| \le \tilde{C}\varepsilon_i\|u(\hat{\mu}_i\hat{\phi}_i)-\hat{u}(\hat{\mu}_i\hat{\phi}_i)\|_1 \ ,$$

where $\tilde{C}$ depends only on γ. The constant in the coercivity bound $\beta_0\|v\|_1^2 \le |||v|||^2$ enters Lemma 4.1 at this final stage. Similarly, a careful reading of the proofs of [26, Lemma 3.4 and 3.5] show that their efficiency results are readily extended to elliptic operators of the type considered here.

Lemma 4.2. *For any $\epsilon>0$, there is a constant $c=c(\epsilon)>0$ depending only on the hp-constant γ and the global continuity constant β_1, such that $\varepsilon_i^2(K) \le cp_K^{2+2\epsilon}|||u(\hat{\mu}_i\hat{\phi}_i)-\hat{u}(\hat{\mu}_i\hat{\phi}_i)|||_{\omega_K}^2$.*

Here, ω_K is the patch of elements which share an edge with K. The global continuity constant β_1 could be replaced in Lemma 4.2 by a local continuity constant $\beta_{1\omega_K}$ if desired.

Remark 4.3. The p-dependence in local efficiency bound of Lemma 4.2 is unfortunately unavoidable in the proof, and would suggest decreased efficiency of the estimator as p_K is increased if this estimate were sharp. Our numerical experiments do seem to indicate that there may be a modest decrease in the efficiency of the estimator under hp-refinement in practical computations.

With these results we now state the main theorem.

Theorem 4.4. *Under the assumptions of Theorem 3.1, we have the following upper- and lower-bounds on eigenvalue error,*

$$C_1 \sum_{i=1}^{\mathrm{M}} \hat{\lambda}_i^{-1} \varepsilon_i^2 \leq \sum_{i=1}^{\mathrm{M}} \frac{\hat{\lambda}_i - \lambda_i}{\hat{\lambda}_i} \leq C_2 \sum_{i=1}^{\mathrm{M}} \hat{\lambda}_i^{-1} \varepsilon_i^2 \ . \tag{23}$$

The constant C_1 depends solely on the ratio $\hat{\lambda}_1/(2\hat{\lambda}_{\mathrm{M}})$, the hp-regularity constant γ, the continuity constant β_1, and the maximal polynomial degree $\bar{p} = \max_{K\in\mathcal{T}} p(K)$. The constant C_2 depends solely on the relative distance to the unwanted component of the spectrum, the hp-regularity constant γ and the coercivity constant β_0.

Proof. These assertions follow directly from Theorem 3.1, Lemma 3.4, and Lemmas 4.1 and 4.2. □

Remark 4.5. It is relative local indicators $\hat{\mu}_i^{-1}\varepsilon_i^2(K)$ which will be used to mark elements for refinement, as will be described in Section 5.

4.1. **Eigenvector estimates.** A similar result holds for the eigenvectors and eigenspaces. Let now

$$E(\lambda_{\mathrm{M}}) = \sum_{\lambda\leq\lambda_{\mathrm{M}},\ \lambda\in\mathrm{Spec}_B} E_\lambda$$

be the L^2 orthogonal projection onto the eigenspace belonging to the first M eigenvalues of the form B as given in Theorem 4.4. Let also $\|\cdot\|_{S_2}$ be the Hilbert-Schmidt norm on the ideal of all Hilbert-Schmidt operators, see [29]. Note that we are considering subsets of the space of bounded (compact) operators from L^2 to L^2. In the matrix analysis the Hilblert-Schmidt norm is known as the Frobenius norm and it can be expressed as $\|A\|_{S_2} = \sqrt{\mathrm{trace}(A^*A)}$, where we have assumed that A is such that $\mathrm{trace}(A^*A)$ is finite. We now have the subspace approximation result.

Theorem 4.6. *Let $\hat{S}_{\mathrm{M}} = \hat{S}_{\mathrm{M}}(\mathcal{T}) = \mathrm{span}(\hat{\phi}_k) \subset V = V(\mathcal{T})$ be the computed approximation of the invariant subspace corresponding to λ_i, $i = 1, \cdots, \mathrm{M}$ and let $\hat{P}(\mathcal{T})$ be the L^2 orthogonal projection onto $\hat{S}_{\mathrm{M}}(\mathcal{T})$. If the assumptions of Theorem 3.1 hold. Then*

$$\|E(\lambda_{\mathrm{M}}) - \hat{P}(\mathcal{T})\|_{S_2} \leq C_{\mathrm{M},\mathcal{T}} \sqrt{\sum_{i=1}^{\mathrm{M}} \hat{\lambda}_i^{-1} \varepsilon_i^2}. \tag{24}$$

The constant $C_{\mathrm{M},\mathcal{T}}$ depends solely on the relative distance to the unwanted component of the spectrum (e.g. $\frac{\lambda_{\mathrm{M}}-\lambda_{\mathrm{M}+1}}{\lambda_{\mathrm{M}}+\lambda_{\mathrm{M}+1}}$), the hp-regularity constant γ and the continuity constant β_1.

Proof. The conclusion follows readily from [19, Theorem 4.2] and Lemmas 3.4 and 4.1. □

This result is a robust reliability estimate which ensures the convergence of invariant subspaces. With additional information on eigenvalue separation we present more detailed efficiency and reliability estimate in an eigenvector setting. Let $\lambda_1 = \lambda_{s_1} < \cdots < \lambda_{s_k}$ be all elements of the set $\{\lambda_i \ : \ i = 1, \cdots, \mathrm{M}\}$. We define the following gap measure

$$\mathrm{Gap}_{\mathrm{M}} := \max_{i\neq j} \frac{\lambda_{s_i} + \lambda_{s_j}}{|\lambda_{s_i} - \lambda_{s_j}|} \ .$$

Theorem 4.7. *Let ψ_i and $\hat{\psi}_i \in V_h^p$, $i = 1, \cdots, \mathrm{M}$ be eigenvectors and Ritz vectors which satisfy both the assumptions of Theorem 3.1 and the paring of Theorem 3.3, that is let $\eta_{\mathrm{M}}(\hat{S}_{\mathrm{M}}) < 1/2 \min\{\mathrm{Gap}_{\mathrm{M}}, \frac{\lambda_{\mathrm{M}}+\lambda_{\mathrm{M}+1}}{\lambda_{\mathrm{M}}-\lambda_{\mathrm{M}+1}}\}$. Then there exist constants C_{V} and c_{V} such that*

$$c_{\mathrm{V}} \sum_{i=1}^{\mathrm{M}} \hat{\lambda}_i^{-1} \varepsilon_i^2 \leq \sum_{i=1}^{\mathrm{M}} \frac{B[\hat{\psi}_i - \psi_i]}{B[\psi_i]} \leq C_{\mathrm{V}} \sum_{i=1}^{\mathrm{M}} \hat{\lambda}_i^{-1} \varepsilon_i^2.$$

The constant $c_{\rm V}$ depends solely on the ratio $\hat{\lambda}_1/(2\hat{\lambda}_2)$, the hp-regularity constant γ, the continuity constant β_1, and the maximal polynomial degree $\bar{p} = \max_{K\in\mathcal{T}} p(K)$. The constant $C_{\rm V}$ depends solely on the relative distance to the unwanted component of the spectrum, the hp-regularity constant γ and the coercivity constant β_0.

Proof. Let us assume that

$$\eta_{\rm M}(\hat{S}_{\rm M}) < 1/2 \min\{\mathrm{Gap}_{\rm M}, \frac{\lambda_{\rm M}+\lambda_{\rm M+1}}{\lambda_{\rm M}-\lambda_{\rm M+1}}\}.$$

Then according to [18, Theorem 6.2] and [20, Proposition 2.5] we may chose eigenvectors ψ_i and Ritz vectors $\hat{\psi}_i$, $i = 1, \cdots, {\rm M}$ such that the paring of Theorem 3.3 holds for every λ_{s_i}, $i = 1, \cdots, k$. Using [20, Proposition 2.5] and [7, Section 4.1] we establish, using the notation from [7, Section 4.1], the estimate

$$\frac{\hat{\lambda}_1}{2\hat{\lambda}_{\rm M}} \sum_{i=1}^{\rm M} \eta_i^2(\hat{S}_m) \leq \sum_{i=1}^{\rm M} \frac{B[\hat{\psi}_i - \psi_i]}{B[\psi_i]} \leq 2\ \mathrm{Gap}_{\rm M} C_{\rm vec} \sum_{i=1}^{\rm M} \eta_i^2(\hat{S}_m).$$

The conclusion of the theorem now follows from Lemmas 3.4, 4.1 and 4.2. □

4.2. **Further references and concluding remarks.** Let us close the theoretical part of the paper by making some comparisons with other works in the literature. Our a posteriori error estimator is based on the consideration of the associated boundary value problems (11) and (12) and so we are able to naturally relate our error estimation technique to the results on the boundary value problem error estimator from [26]. Any improvement in the analysis of the boundary value approximation error estimator will readily lead to the improvement of our estimator.

A further claim to this end are results like Theorem 3.3 which indicate that the underlying ideal continuous eigenvalue approximation error estimator is asymptotically exact. The computable error estimator ε_i^2 is expected to better replicate its behavior as asymptotically sharper estimators of the associated boundary value problem become available. Our eigenvalue/eigenvector estimation frameworks is such that any boundary value error estimator can be readily included providing a result like Lemmas 4.1 and 4.2 exist.

A similar eigenvalue/eigenvector approximation error estimator, also based on the estimator from [26], has been presented in [4]. In comparison we provide a more robust analysis of the reliability of the eigenvalue/eigenvector estimator (results from [4] were primarily for single eigenvalues, cf [4, Proposition 3.1]). Furthermore, our analysis provides error estimates for the multiple and clustered eigenvalues where stability of the estimates depends only on the separation of a multiple eigenvalue (cluster of eigenvalues) from the rest of the spectrum. Note that multiple or clustered eigenvalues appear as result of symmetries or near symmetries of the problem and are a typical feature of 2D or 3D eigenvalue problems.

As has been pointed out in [4], lower (the so called efficiency) estimates of the error are still suboptimal (cf. Remark 4.3 and the lower estimate c_V from Theorem 4.7) in the sense that the lower "error equivalence" constants depend on the maximal polynomial degree of the approximating *hp* finite element space. As a consequence, we do not use our estimator to decide on the p refinement. To decide on the choice between h and p refinements we use the technique of estimating the local analyticity of the solution as described in [14, 21], for further discussion see Section 5.

5. Benchmarks

In the numerical experiments we illustrate the efficiency of the estimator (23) on several problems of the general form

$$\mathcal{L}\psi = \lambda\psi \text{ in } \Omega \quad , \quad \|\psi\| = 1 \ , \tag{25}$$

for a second-order, linear elliptic operator $\mathcal{L}$, where homogeneous Dirichlet or Neumann conditions are imposed on the boundary. We then proceed to give benchmark results for eigenvalues which are accompanied by the eigenvector approximation estimates. We do not report timing, since a discontinuous Galerkin method is mostly computationally more efficient at the expense of less robust error estimation theory.

Following [6], we assume an error model of the form

$$\hat{\lambda}_i = \lambda_i + Ce^{-2\alpha\sqrt{\mathrm{DOFs}}}$$

for problems whose eigenvectors are expected to be smooth, and

$$\hat{\lambda}_i = \lambda_i + Ce^{-2\alpha\sqrt[3]{\text{DOFs}}},$$

for problems such as those on non-convex polygonal domains and/or discontinuous coefficients, whose eigenvectors are expected to have isolated singularities. We use DOFs $= \dim(V_k^p)$ to denote the size of the discrete problem. The constants C and α are determined by least-squares fitting, and α is reported for each problem. Plots are given of the total relative error, its *a posteriori* estimate, and the associated effectivity index, shown, respectively, below:

$$\sum_{i=1}^{\text{M}} \frac{\hat{\lambda}_i - \lambda_i}{\hat{\lambda}_i} \quad , \quad \sum_{i=1}^{\text{M}} \hat{\lambda}_i^{-1}\varepsilon_i^2 \quad , \quad \frac{\sum_{i=1}^{\text{M}} \frac{\hat{\lambda}_i - \lambda_i}{\hat{\lambda}_i}}{\sum_{i=1}^{\text{M}} \hat{\lambda}_i^{-1}\varepsilon_i^2} \ .$$

In the case of a single eigenvalue λ_i the effectivity index reduces $(\hat{\lambda}_i - \lambda_i)/\varepsilon_i^2$, and we make the following comparison with what is presented in [4], in which *hp*-adaptivity is also used for eigenvalue problems. The effectivities reported in [4] are in terms of eigen*function* error, which corresponds closely with the square root of the effectivities reported here. This difference should be taken into consideration when comparing the effectivities reported here with those in [4] or other similar contributions. For problems in which the exact eigenvalues are known, we use these values in our error analysis. For most problems, we use highly accurate computations on very large problems to produce "exact eigenvalues" for our comparisons, as discussed in the introduction.

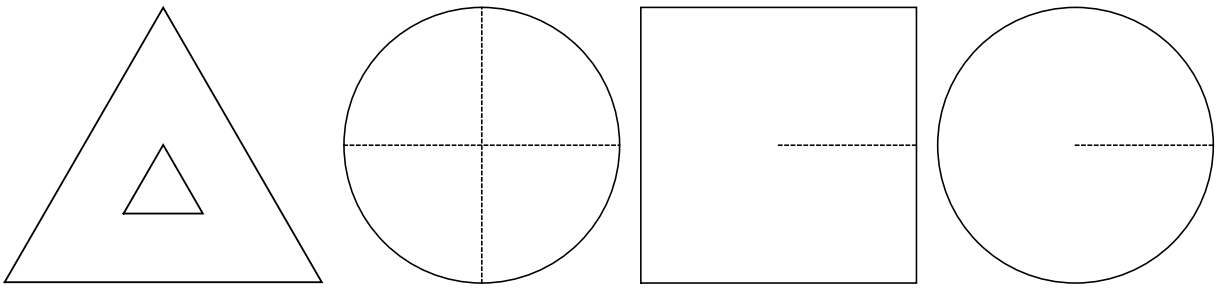

FIGURE 1. Some of the domains under consideration.

In all simulations we used an *hp*-adaptive algorithm in order to get the best convergence possible. To drive the *hp*-adaptivity we use the element-wise contributions to the quantity $\sum_{i=1}^{\text{M}} \hat{\lambda}_i^{-1}\varepsilon_i^2$, to provide local error indicators. Then, we apply a simple fixed-fraction strategy to mark the elements to adapt. For each marked element, the choice of whether to locally refine it or vary its approximation order is made by estimating the local analyticity of the computed eigenvectors in the interior of the element by computing the coefficients of the L^2-orthogonal polynomial expansion (cf. [14]).

5.1. **Dirichlet Laplacian on the Unit Triangle.** As a simple problem for which the eigenvalues and eigenvectors are explicitly known (cf. [25]), we consider the problem where: $\mathcal{L} = -\Delta$, Ω is equilateral triangle of having unit edge-length, and $\psi = 0$ on $\partial\Omega$. The eigenvalues can be indexed as

$$\lambda_{mn} = \frac{16\pi^2}{9}(m^2 + mn + n^2) \ ,$$

and we refer interested readers to [25] for explicit descriptions of the eigenvectors.

In Figure 2 we plot the total relative error for the first four eigenvalues, together with the associated error estimate; and in Figure 3 we plot the effectivity quotient. In this case we have obtained $\alpha = 0.5070$. It is clear that the convergence is exponential in this case, and that the effectivity undergoes a mild degradation as the problem size increases. This modest decrease in effectivity is in line with Remark 4.3, and it is also seen in several of our remaining experiments.

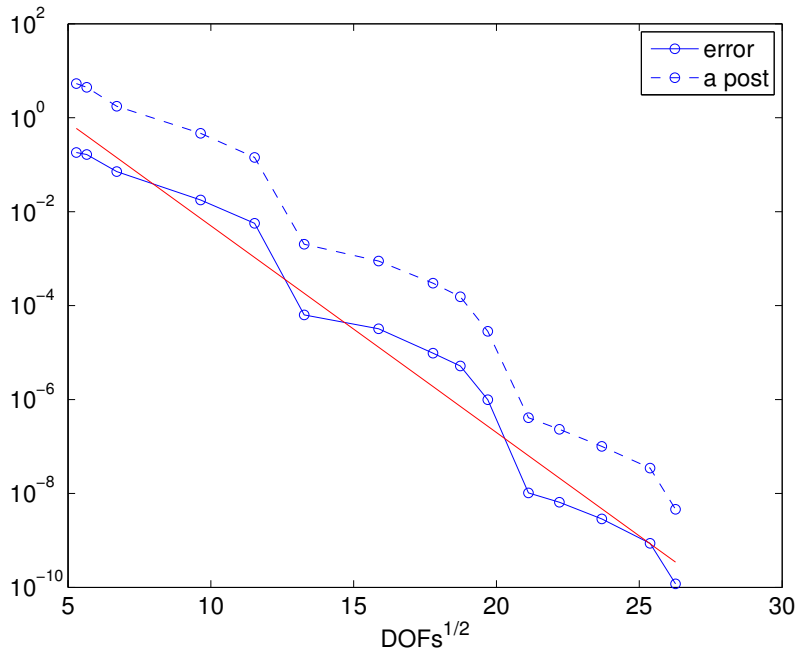

FIGURE 2. Triangle Problem: Total relative errors and *a posteriori* estimates for the first four eigenvalues. The solid line corresponds to the error model $Ce^{-2\alpha\sqrt{DOFs}}$, with $\alpha = 0.5070$.

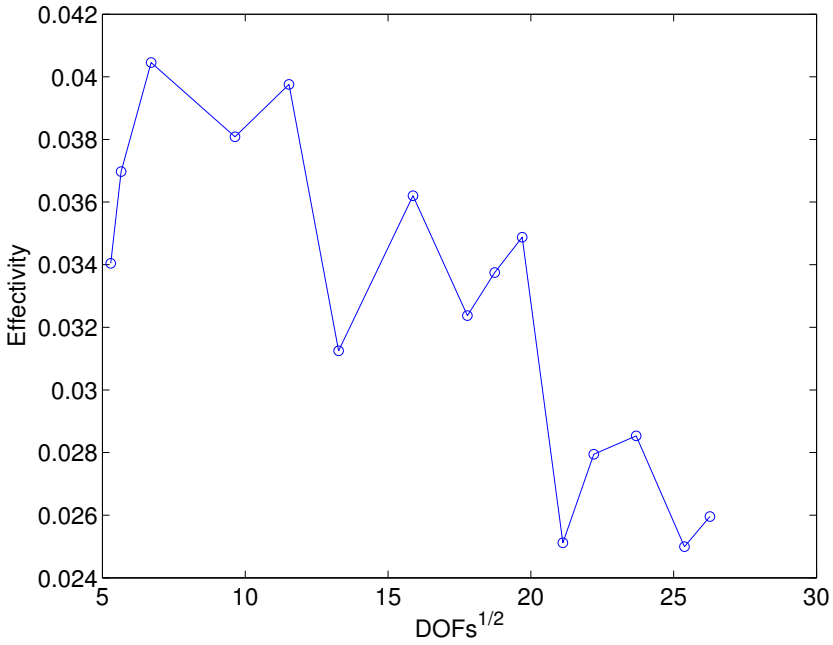

FIGURE 3. Triangle Problem: Effectivity indices.

5.2. **Dirichlet Laplacian on the Unit Triangle with on a Hole.** We now consider the problem where $\mathcal{L} = -\Delta$, Ω is the equilateral triangle having edge-length 2 with an equilateral triangle having edge-length 1/2 removed from its center (see Figure 1), and $\psi = 0$ on $\partial\Omega$. For such a problem, it is expected that some

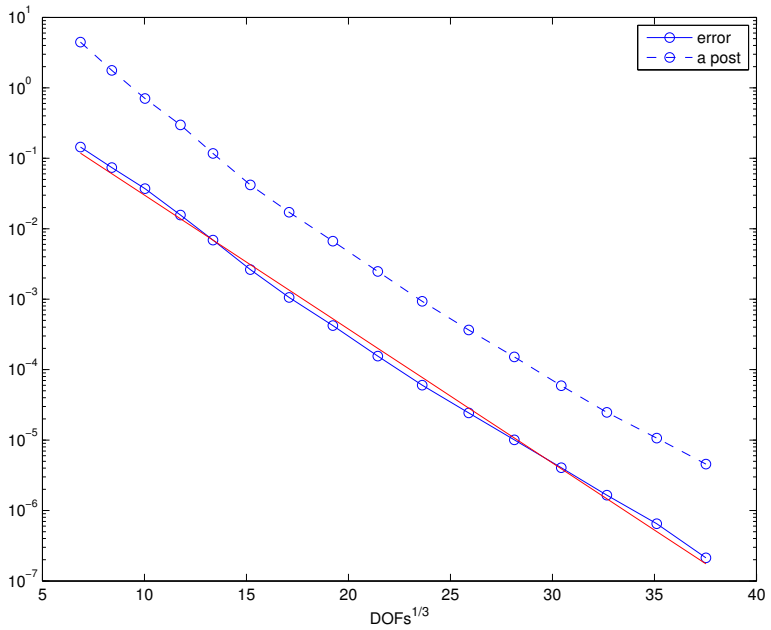

FIGURE 4. Triangle with Hole: Total relative errors and *a posteriori* estimates for the first three eigenvalues. The solid line corresponds to the error model $Ce^{-2\alpha\sqrt[3]{DOFs}}$, with $\alpha = 0.2190$

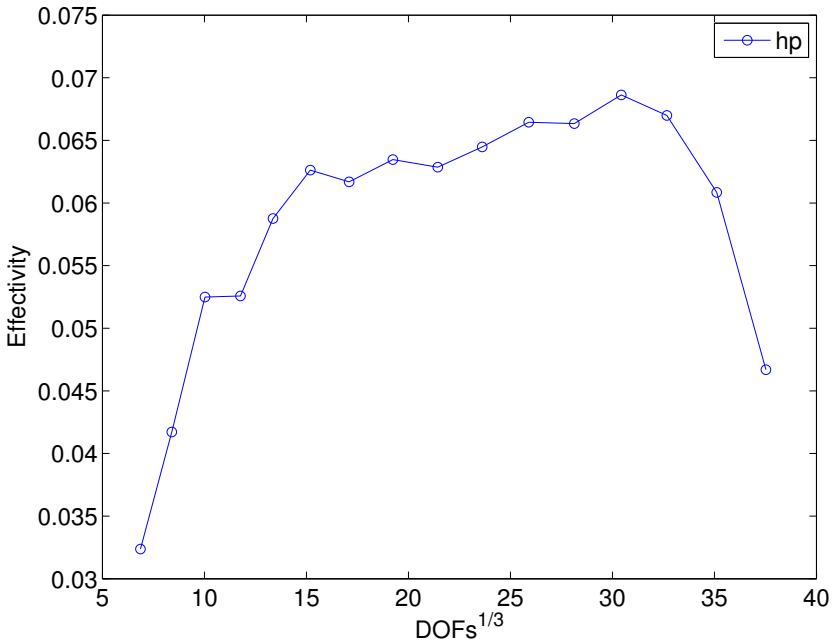

FIGURE 5. Triangle with Hole: Effectivity indices

of the eigenvectors will have an $r^{3/5}$-type singularity at each of the three interior corners, where r is the distance to the nearest corner. In this case, the exact eigenvalues are unknown, so we computed the following reference values of them on a very large problem: 40.4650426 for the first eigenvalue and 43.4868466 for the second and third, which form a double eigenvalue. These values are accurate at least up to 1e-6.

In Figure 4 we plot the relative error and error estimates together, for the first three eigenvalues, and in Figures 5 we plot the corresponding values of the effectivity quotient. We again see exponential convergence with $\alpha = 0.2190$ and a modest deterioration of effectivity.

5.3. **Square Domain with Discontinuous Reaction Term.** For this pair of problems we take $\Omega = (0,1)^2$, $\nabla\psi \cdot \mathbf{n} = 0$ on $\partial\Omega$, and $\mathcal{L}\,\psi = -\Delta\psi + \kappa V_{MD} \cdot \psi$, where V_{MD} is the characteristic function of the touching squares labelled $\mathcal{M}_1$ in Figure 6. We consider two values of the constant parameter, $\kappa = 10, 100$. It is straightforward to see that the corresponding bilinear form is an inner-product in this case (no zero eigenvalues), and that all eigenvectors are at least in H^2.

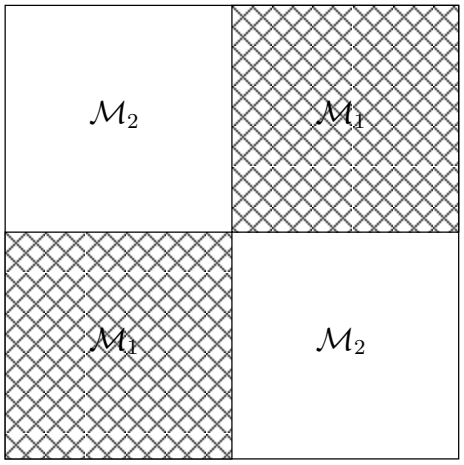

FIGURE 6. A modification of the touching squares example of M. Dauge.

For $\kappa = 10$, we have in Figure 7 the total relative error and error estimates for the first four eigenvalues; and the effectivity quotient is given in Figure 8. For these simulations we used the following reference values for the first four eigenvalues, which are 1e-8 accurate: 4.150242455, 10.706070962, 18.779725462, 25.150325247. The analogous plots for the first four eigenvalues in the case $\kappa = 100$ are given in Figure 9 and Figure 10. For these simulations, we used the following reference values for the first four eigenvalues, which are 1e-8 accurate: 13.210576406, 13.990033964, 60.294151672, 64.840268299. In both cases we see apparent exponential convergence with $\alpha = 0.2495$ and $\alpha = 0.1827$ respectively, and reasonable effectivity behavior. It is clear from the error plots that for both values of κ the convergence is exponential.

5.4. **Square Domain with Discontinuous Diffusion Term.** Using the domain $\Omega = (0,1)^2$, partitioned into regions $\mathcal{M}_1$ and $\mathcal{M}_2$ as in Figure 6, and homogeneous Dirichlet conditions $\psi = 0$ on $\partial\Omega$, we consider the operator $\mathcal{L} = -\nabla \cdot (a\nabla)$, where $a = 1$ in $\mathcal{M}_2$ and $a = \kappa$ in $\mathcal{M}_1$. Such problems can have arbitrarily bad singularities at the cross-point of the domain depending on the relative sizes of a in the two subdomains—see, for example, [22, 23, 11, 12] and [27, Example 5.3].

We have considered two values for κ in $\mathcal{M}_1$: 10 and 100. Since the exact eigenvalues are not available, we computed the following three reference values for the first three eigenvalues when $\kappa = 10$: 64.226529416, 75.028156269, 141.161506328; and the following three reference values for the first three eigenvalues when $\kappa = 100$: 77.800981966, 78.564198245, 193.916538067. All reference values are at least 1e-8 accurate. The relative error and effectivity plots for both cases are given in Figures 11-14, and again we see apparent exponential convergence with $\alpha = 0.5630$ and $\alpha = 0.5669$ respectively. Moreover in Figure 15 we reported the final mesh and the final distribution of polynomials orders for $\kappa = 100$.

5.5. **A Kellogg Problem.** We here consider a variant of the previous problem type for which we can give more specific information about the kinds of singularities which can be expected in terms of the size of the jump discontinuity. More specifically, we consider problems of the form

$$\int_\Omega a\nabla\psi \cdot \nabla v \, dx = \lambda \int_\Omega a\psi v \, dx \ , \tag{26}$$

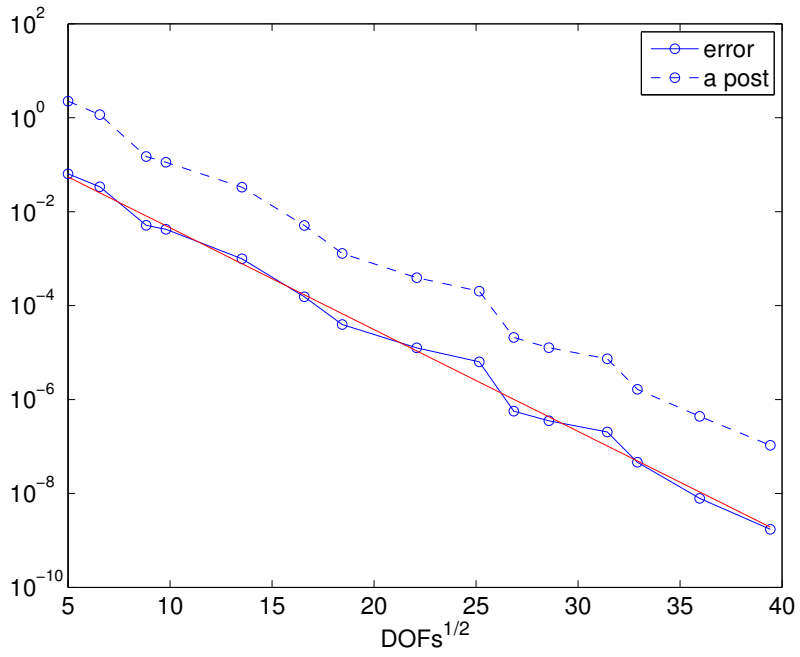

FIGURE 7. Square Domain, Discontinuous Reaction Term, $\kappa = 10$: Total relative errors and *a posteriori* estimates for the first four eigenvalues. The solid line corresponds to the error model $Ce^{-2\alpha\sqrt{DOFs}}$, where $\alpha = 0.2495$.

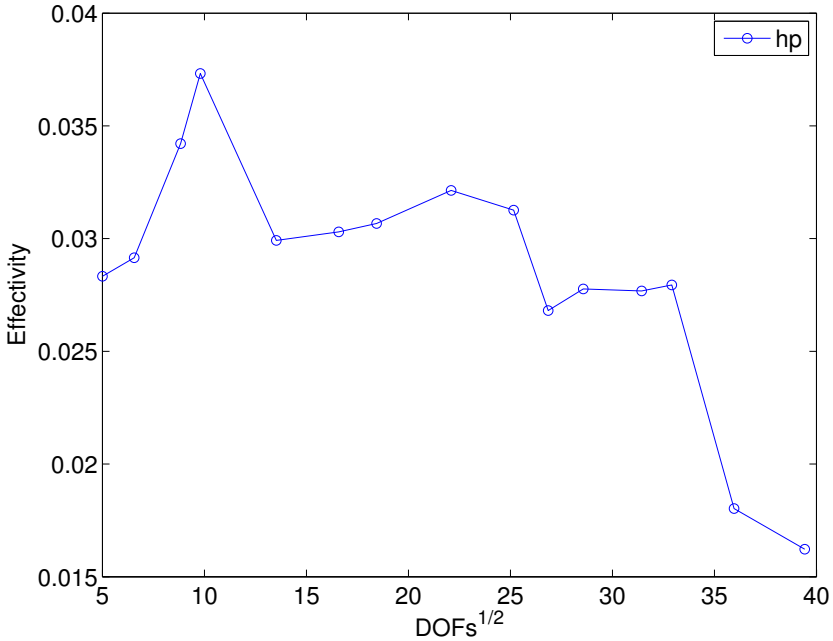

FIGURE 8. Square Domain, Discontinuous Reaction Term, $\kappa = 10$: Effectivity indices.

where a has jump discontinuities across certain internal interfaces. We refer to this type of problem (26) as a *Kellogg eigenvalue problem*, in reference to the work of that author on boundary value problems of this sort—although an argument could be made for calling the previous problem type by this name.

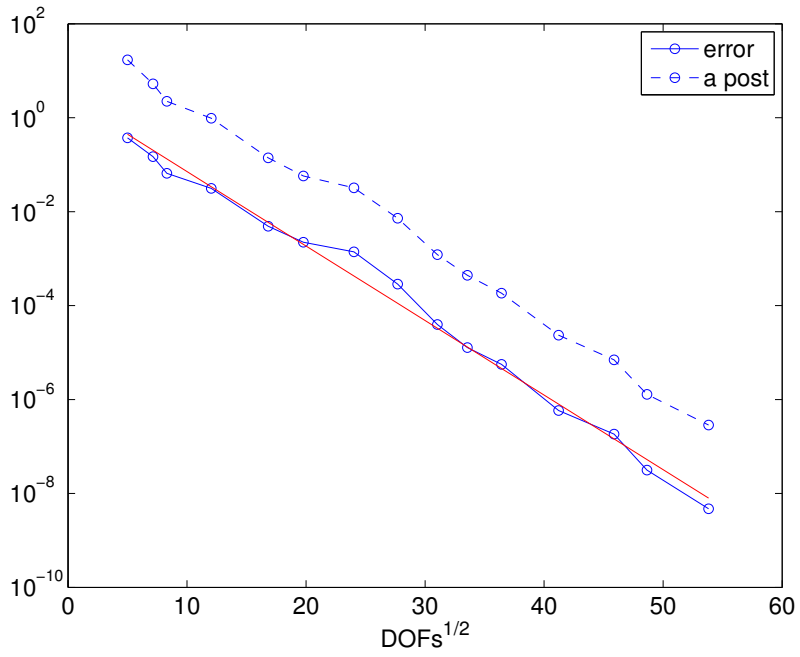

FIGURE 9. Square Domain, Discontinuous Reaction Term, $\kappa = 100$: Total relative errors and *a posteriori* estimates for the first four eigenvalues. The solid line corresponds to the error model $Ce^{-2\alpha\sqrt{DOFs}}$, where $\alpha = 0.1827$.

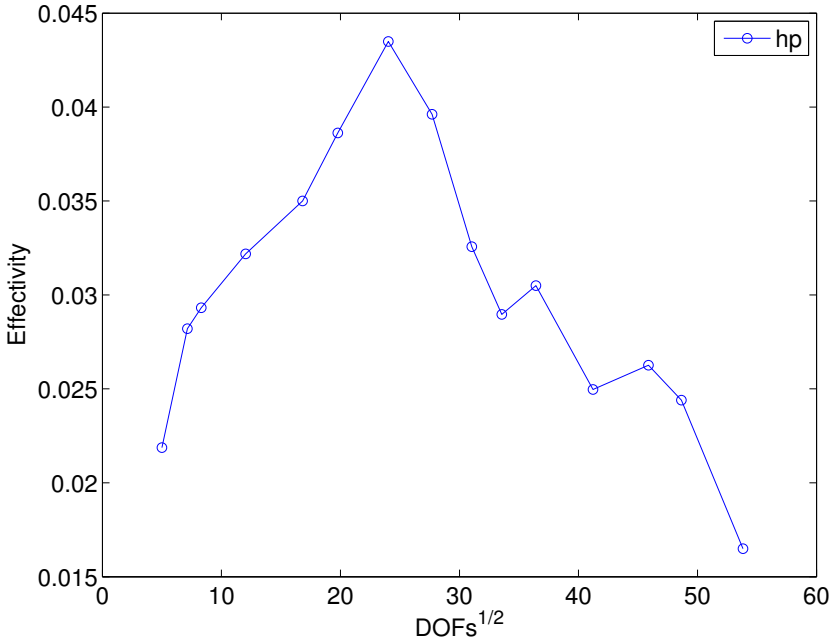

FIGURE 10. Square Domain, Discontinuous Reaction Term, $\kappa = 100$: Effectivity indices.

If Ω is the unit disk and $a = \kappa = \beta^2$ in the first and third quadrants, and $a = 1$ in the second and fourth quadrants (see Figure 1), we can describe the eigenpairs explicitly. We assume that $\beta > 1$. The eigenvalues and functions can be split into three different classes, which we now describe.

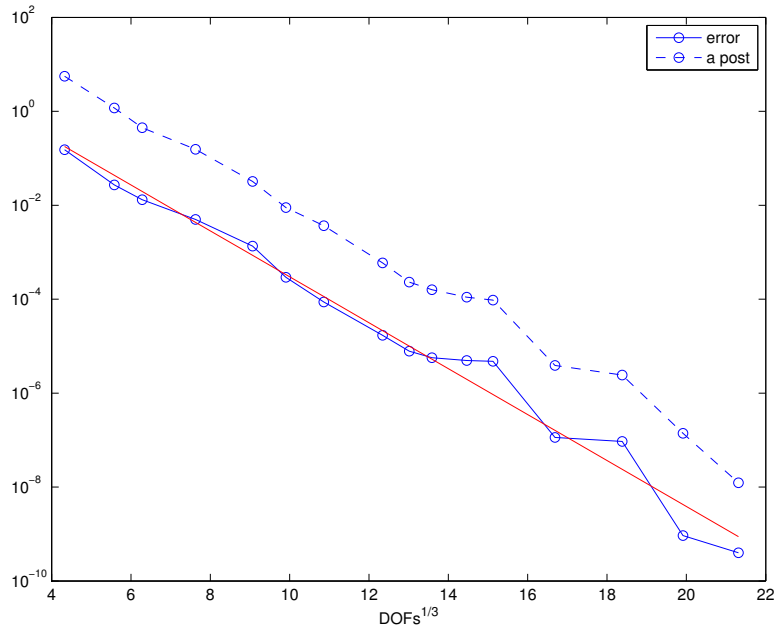

FIGURE 11. Square Domain, Discontinuous Diffusion Term, $\kappa = 10$: Total relative errors and *a posteriori* estimates for the first three eigenvalues. The solid line corresponds to the error model $Ce^{-2\alpha\sqrt[3]{DOFs}}$, where $\alpha = 0.5630$.

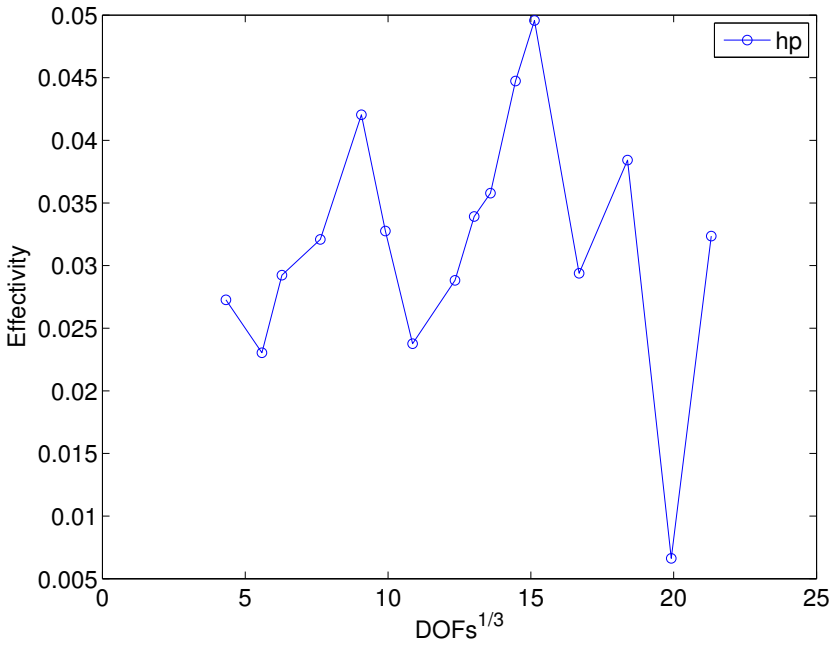

FIGURE 12. Square Domain, Discontinuous Diffusion Term, $\kappa = 10$: Effectivity indices.

Class 1. For $k \geq 0$ and $m \geq 1$, let $z_{km}^{(1)}$ be the m^{th} positive root of the first-kind Bessel function J_{2k}. The eigenvalues of this class are $\lambda_{km}^{(1)} = (z_{km}^{(1)})^2$, and each of them, with the exception of those for $k = 0$, are

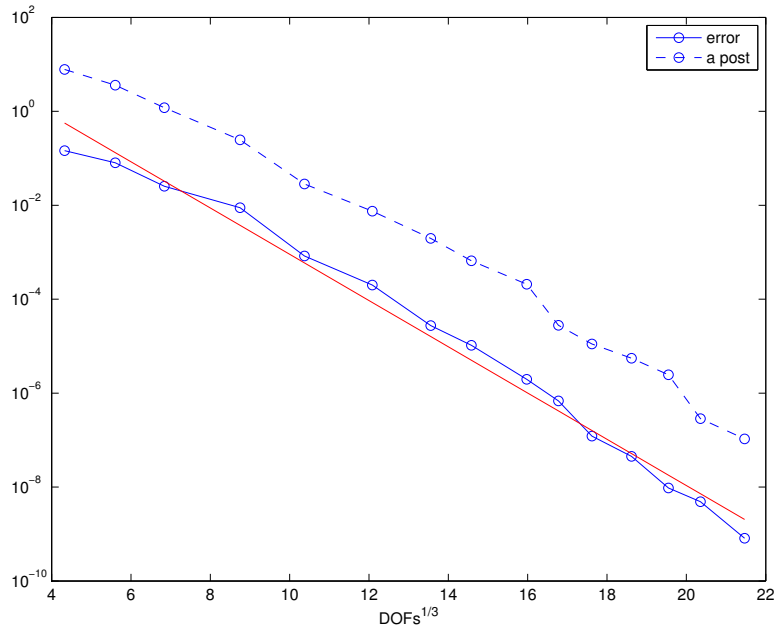

FIGURE 13. Square Domain, Discontinuous Diffusion Term, $\kappa = 100$: Total relative errors and *a posteriori* estimates for the first three eigenvalues. The solid line corresponds to the error model $Ce^{-2\alpha\sqrt[3]{DOFs}}$, where $\alpha = 0.5669$.

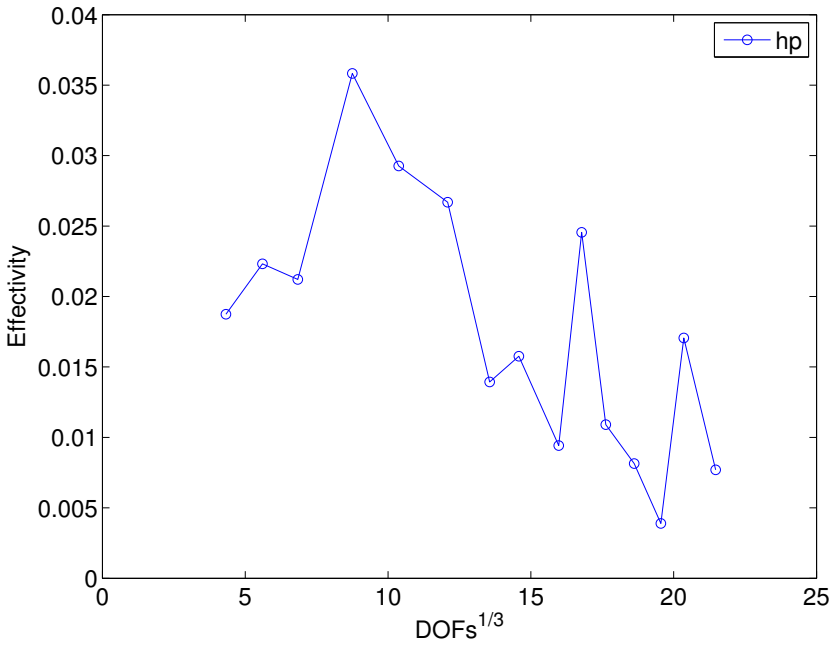

FIGURE 14. Square Domain, Discontinuous Diffusion Term, $\kappa = 100$: Effectivity indices.

double-eigenvalues. The corresponding eigenvectors are

$$\psi_{km}^{(1)} = J_{2k}(z_{km}^{(1)} r)\cos(2k\theta) \quad , \quad \Psi_{km}^{(1)} = a^{-1/2} J_{2k}(z_{km}^{(1)} r)\sin(2k\theta) \ .$$

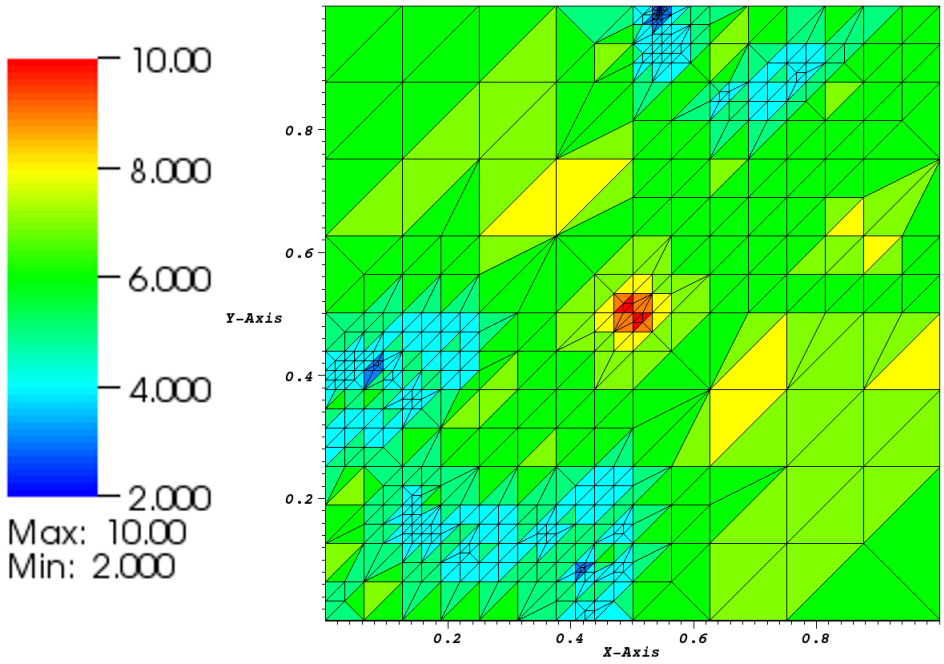

FIGURE 15. Square Domain, Discontinuous Diffusion Term, $\kappa = 100$: Final mesh and order of polynomials for the central region of the domain (the region of the singularity).

Obviously, $\Psi^{(1)}_{km}$ is discarded when $k = 0$. We see that the eigenvalues of this type are independent of β, as are the eigenvectors $\psi^{(1)}_{km}$, which are analytic. On the other hand, eigenvectors $\Psi^{(1)}_{km}$ do depend on β.
Class 2. For $k \geq 0$ and $m \geq 1$, let $z^{(2)}_{km}$ be the m^{th} positive root of the first-kind Bessel function J_{σ_k}, where $\sigma_k = 2k + \frac{4}{\pi}\text{arccot}(\beta)$. The eigenvalues are $\lambda^{(2)}_{km} = (z^{(2)}_{km})^2$, and the corresponding eigenvectors are $\psi^{(2)}_{km} = a^{-1/2} J_{\sigma_k}(z^{(2)}_{km} r)\, g_k(\theta)$, where

$$g_k(\theta) = \begin{cases} -\cos(\sigma_k(\pi/4 - \theta)) & , \theta \in [0, \pi/2) \\ -\sin(\sigma_k(3\pi/4 - \theta)) & , \theta \in [\pi/2, \pi) \\ \cos(\sigma_k(5\pi/4 - \theta)) & , \theta \in [\pi, 3\pi/2) \\ \sin(\sigma_k(7\pi/4 - \theta)) & , \theta \in [3\pi/2, 2\pi) \end{cases} \quad \text{when } k \text{ is even ,}$$

$$g_k(\theta) = \begin{cases} -\sin(\sigma_k(\pi/4 - \theta)) & , \theta \in [0, \pi/2) \\ -\cos(\sigma_k(3\pi/4 - \theta)) & , \theta \in [\pi/2, \pi) \\ \sin(\sigma_k(5\pi/4 - \theta)) & , \theta \in [\pi, 3\pi/2) \\ \cos(\sigma_k(7\pi/4 - \theta)) & , \theta \in [3\pi/2, 2\pi) \end{cases} \quad \text{when } k \text{ is odd .}$$

Class 3. For $k \geq 1$ and $m \geq 1$, let $z^{(3)}_{km}$ be the m^{th} positive root of the first-kind Bessel function J_{ρ_k}, where $\rho_k = 2k - \frac{4}{\pi}\text{arccot}(\beta)$. The eigenvalues are $\lambda^{(3)}_{km} = (z^{(3)}_{km})^2$, and the corresponding eigenvectors are

$\psi_{km}^{(3)} = a^{-1/2} J_{\rho_k}(z_{km}^{(3)} r)\, h_k(\theta)$, where

$$h_k(\theta) = \begin{cases} \cos(\rho_k(\pi/4-\theta)) & , \theta \in [0,\pi/2) \\ -\sin(\rho_k(3\pi/4-\theta)) & , \theta \in [\pi/2,\pi) \\ -\cos(\rho_k(5\pi/4-\theta)) & , \theta \in [\pi,3\pi/2) \\ \sin(\rho_k(7\pi/4-\theta)) & , \theta \in [3\pi/2,2\pi) \end{cases} \quad \text{when } k \text{ is even ,}$$

$$h_k(\theta) = \begin{cases} \sin(\rho_k(\pi/4-\theta)) & , \theta \in [0,\pi/2) \\ -\cos(\rho_k(3\pi/4-\theta)) & , \theta \in [\pi/2,\pi) \\ -\sin(\rho_k(5\pi/4-\theta)) & , \theta \in [\pi,3\pi/2) \\ \cos(\rho_k(7\pi/4-\theta)) & , \theta \in [3\pi/2,2\pi) \end{cases} \quad \text{when } k \text{ is odd .}$$

It is clear from these expressions that singularities of type r^γ for any $\gamma \in (0,1)$ may be achieved by choosing β large enough—these may be obtained by Class 2 eigenvectors when $k = 0$, for example.

If we choose $\kappa = \beta^2 = 10$ for the circle domain, the eigenvectors associated with the smallest three eigenvalues are

$$\begin{aligned} \psi_{01}^{(1)} &= J_0(z_{01}^{(1)} r) & z_{01}^{(1)} &\approx 2.404825557695772768621631879 33 \\ \psi_{01}^{(2)} &= a^{-1/2} J_{\sigma_0}(z_{01}^{(2)} r)\, g_0(\theta) & z_{01}^{(2)} &\approx 2.984417164933079597859305 5397 \\ \psi_{11}^{(3)} &= a^{-1/2} J_{\rho_1}(z_{11}^{(3)} r)\, h_1(\theta) & z_{11}^{(3)} &\approx 4.636195897734832181273430 87762 \end{aligned}$$

The second of these has an r^{σ_0}-type singularity at the origin, where $\sigma_0 \approx 0.389964$; the third of these has an r^{ρ_1}-type singularity at the origin, where $\rho_1 \approx 1.61004$. So it is clear that the second eigenvector is the most singular.

We compute eigenvalues on the analogous square domain (Figure 6), with $a = 1$ in $\mathcal{M}_2$ and $a = \kappa = \beta^2 = 10$ in $\mathcal{M}_1$. The singular behavior of the eigenvectors near the cross point will be the same as for the circular domain. In Figures 16-17 we report the total relative error and error estimates for the first three eigenvalues, and the effectivity index. For these simulations we used the following reference values for the first three eigenvalues: 19.739208802 (1e-8), 30.264820 (1e-5), 70.310149038 (1e-8). Again we see apparent exponential convergence, with $\alpha = 0.2624$.

5.6. **Square Domain with a Slit.** For this problem, $\mathcal{L} = -\Delta$ and $\Omega = (0,1)^2 \setminus S$, where $S = \{(x, 1/2) : 1/2 \le x \le 1\}$; this is pictured in Figure 1, with S as the dashed segment. Homogeneous Neumann conditions are imposed on both "sides" of S and homogeneous Dirichlet boundary conditions are imposed on the rest of the boundary of Ω. For this example we used the following reference values for the first four eigenvalues, with accuracies given in parentheses: 20.739208802 (1e-8), 34.485320 (1e-5), 50.348022005 (1e-8), 67.581165196 (1e-8).

To give some indication of the nature of the eigenvectors in the interior, we briefly consider a related problem where Ω is the unit disk with a slit along the positive x-axis, as pictured in Figure 1, with the same boundary conditions. In this case, the eigenvalues and eigenvectors are known explicitly. For $k \ge 0$ and $m \ge 1$, let z_{km} be the m^{th} positive root of the first-kind Bessel function $J_{k/2}$. It is straightforward to verify that, up to renormalization of eigenvectors, the eigenpairs can be indexed by

$$\lambda_{km} = z_{km}^2 \quad , \quad \psi_{km} = J_{k/2}(z_{km} r)\cos(k\theta/2) \quad , \quad k \ge 0\ ,\ m \ge 1\ .$$

We see that $\psi_{km} \sim \cos(k\theta/2)\left(\frac{z_{km} r}{2}\right)^{k/2}$ as $r \to 0$, so singularities of type $r^{k/2}$ occur infinitely many times in the spectrum. The strongest of these singularities is of type $r^{1/2}$, and it occurs in the eigenvector associated with the second eigenvalue, for example. The same asymptotic behavior of the eigenvectors near the crack tip is expected for the square and circular domains, and in Figure 18 we show a contour plot of the second eigenvalue for the square domain.

In Figure 19 we plot the total relative errors and error estimates for the first four eigenvalues with $\alpha = 0.3314$, and in Figure 20 the individual eigenvalue errors are shown. It is clear from the second of these figures that the second eigenvalue, which corresponds to the most singular eigenvector, clearly has the worst convergence rate (as expected), and that this is what "spoils" the convergence of the cluster of the first four eigenvalues. This becomes even more apparent when Figure 21 (with $\alpha = 0.3121$), which corresponds to

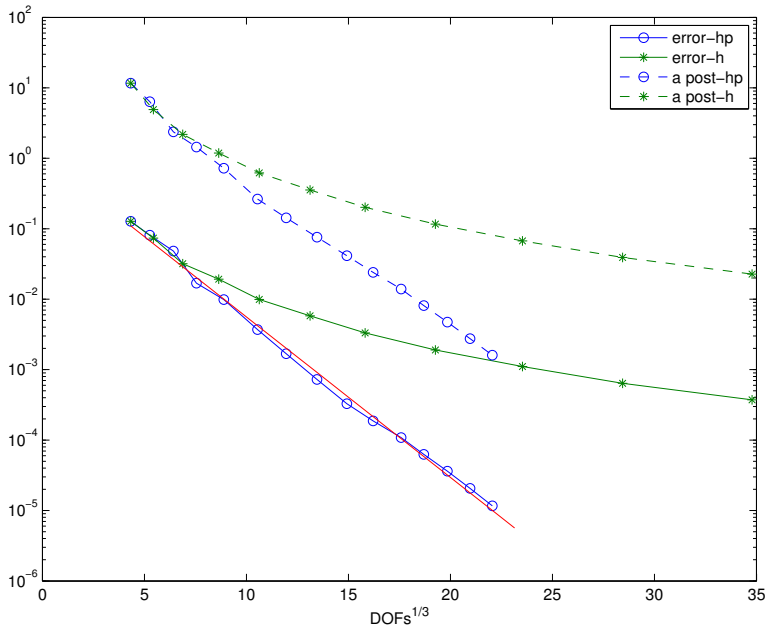

FIGURE 16. Kellogg Problem on Square Domain, $\kappa = 10$: Total relative errors and *a posteriori* estimates for the first three eigenvalues. The solid line corresponds to the error model $Ce^{-2\alpha\sqrt[3]{DOFs}}$, where $\alpha = 0.2642$. We also include the analogous data for pure h-adaptive refinement using quadratic elements to illustrate the difference in performance from the hp version.

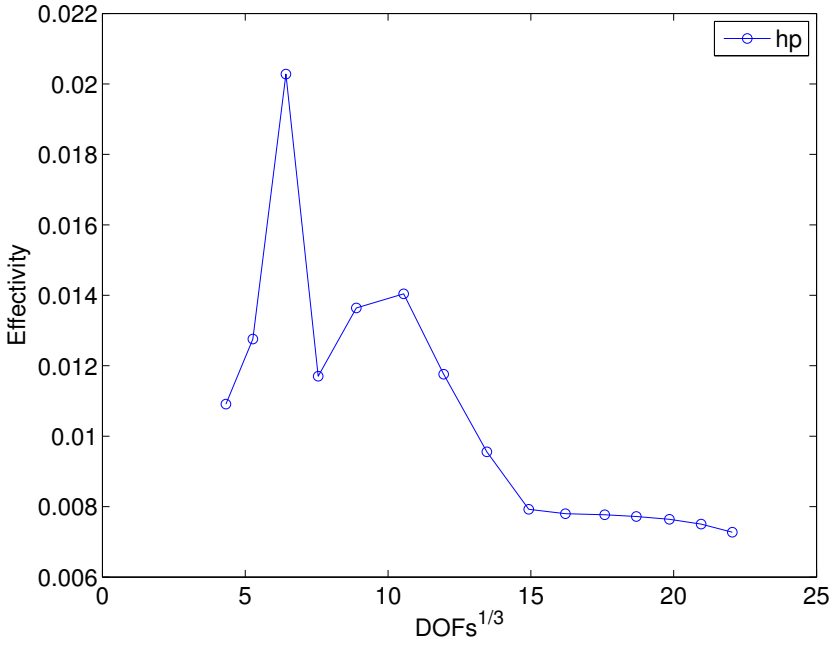

FIGURE 17. Kellogg Problem on Square Domain, $\kappa = 10$: Effectivity indices.

the second eigenvalue alone, is compared with Figure 19—they are nearly identical. Moreover in Figures 22

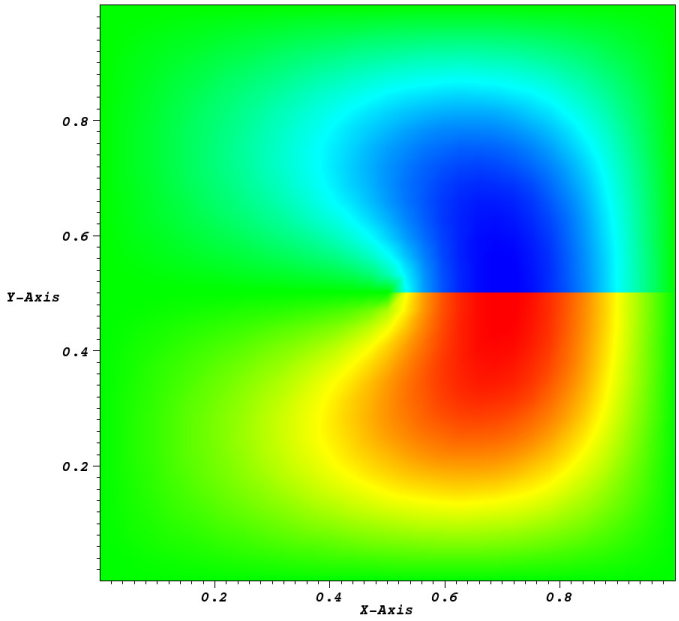

FIGURE 18. Square Domain with Neumann-Neumann Slit: Contour plot of second eigenvector.

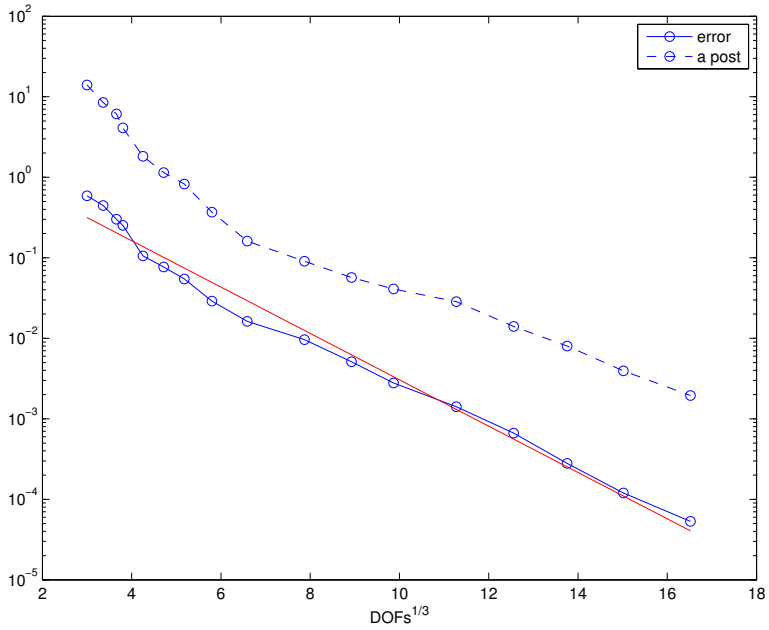

FIGURE 19. Square Domain with Neumann-Neumann Slit: Total relative errors and *a posteriori* estimates for first four eigenvalues. The solid line corresponds to the error model $Ce^{-2\alpha\sqrt[3]{DOFs}}$, where $\alpha = 0.3314$.

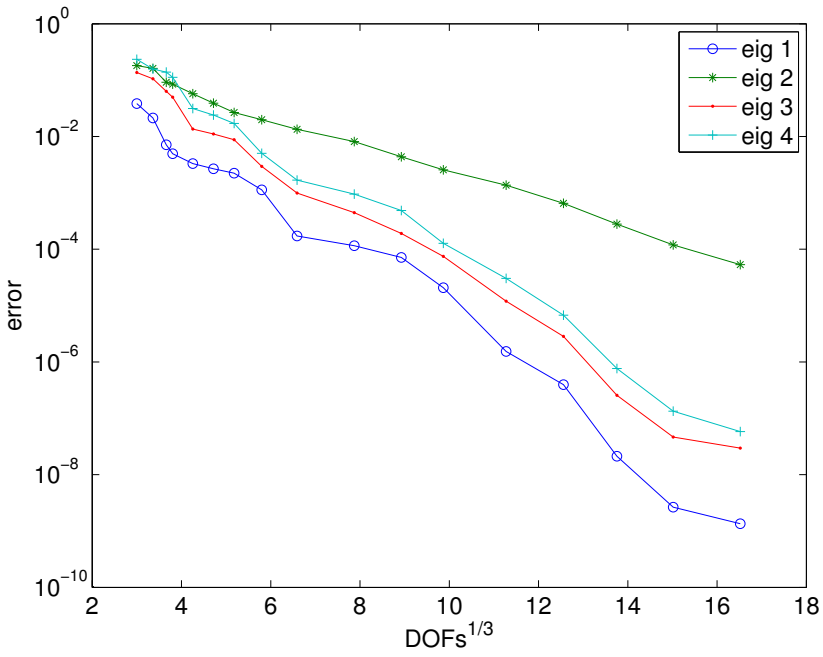

FIGURE 20. Square Domain with Neumann-Neumann Slit: Relative errors for each of the first four eigenvalues individually.

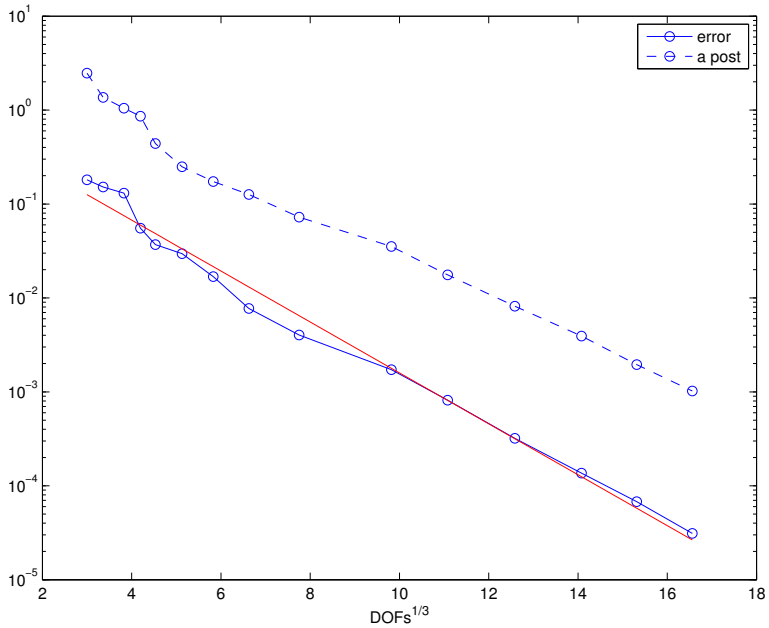

FIGURE 21. Square Domain with Neumann-Neumann Slit: Relative errors and *a posteriori* estimates for the second eigenvalue only. The solid line corresponds to the error model $Ce^{-2\alpha\sqrt[3]{DOFs}}$, where $\alpha = 0.121$.

and 23 we report the final mesh and the final distribution of polynomials orders for the second eigenvalue. As can be seen, the adaptive procedure has automatically heavily refined in the center, where the singularity is located.

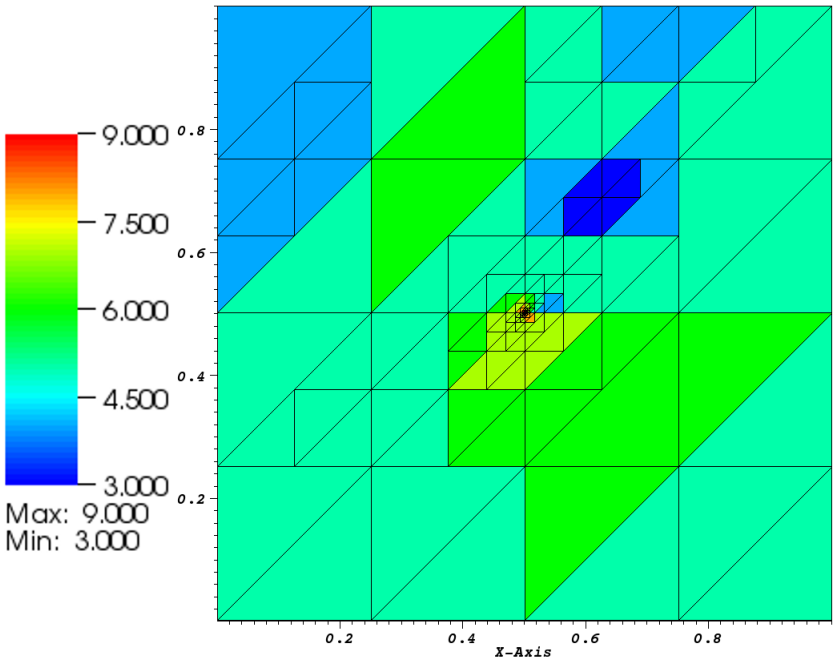

FIGURE 22. Square Domain with Neumann-Neumann Slit: Final mesh and order of polynomials for the second eigenvalue only.

ACKNOWLEDGEMENTS

The work of L. Grubišić was supported by the grant: "Spectral decompositions – numerical methods and applications", Grant Nr. 037-0372783-2750 of the Croatian MZOS. The authors thank anonymous reviewers for their valuable comments which improved the presentation of the paper.

REFERENCES

[1] H. AMMARI, Y. CAPDEBOSCQ, H. KANG, AND A. KOZHEMYAK, *Mathematical models and reconstruction methods in magneto-acoustic imaging*, European J. Appl. Math., 20 (2009), pp. 303–317.

[2] H. AMMARI, H. KANG, E. KIM, AND H. LEE, *Vibration testing for anomaly detection*, Math. Methods Appl. Sci., 32 (2009), pp. 863–874.

[3] H. AMMARI, H. KANG, AND H. LEE, *Asymptotic analysis of high-contrast phononic crystals and a criterion for the band-gap opening*, Arch. Ration. Mech. Anal., 193 (2009), pp. 679–714.

[4] M. G. ARMENTANO, C. PADRA, R. RODRÍGUEZ, AND M. SCHEBLE, *An hp finite element adaptive scheme to solve the Laplace model for fluid-solid vibrations*, Comput. Methods Appl. Mech. Engrg., 200 (2011), pp. 178–188.

[5] M. AZAÏEZ, M. O. DEVILLE, R. GRUBER, E. H. MUND, *A new hp method for the* $-\text{grad}(\text{div})$ *operator in non-Cartesian geometries*, Appl. Numer. Math., 58 (2008), pp. 985–998.

[6] I. BABUŠKA AND B. Q. GUO, *The h-p version of the finite element method for domains with curved boundaries*, SIAM Journal on Numerical Analysis, 25 (1988), pp. 837–861.

[7] R. BANK, L. GRUBIŠIĆ, AND J. S. OVALL, *A framework for robust eigenvalue and eigenvector error estimation and ritz value convergence enhancement*, Applied Numerical Mathematics, Volume 66 (2013), pp. 1–29.

[8] A. H. BARNETT AND T. BETCKE, *Stability and convergence of the method of fundamental solutions for Helmholtz problems on analytic domains*, J. Comput. Phys., 227 (2008), pp. 7003–7026.

[9] T. BETCKE, *A GSVD formulation of a domain decomposition method for planar eigenvalue problems*, IMA J. Numer. Anal., 27 (2007), pp. 451–478.

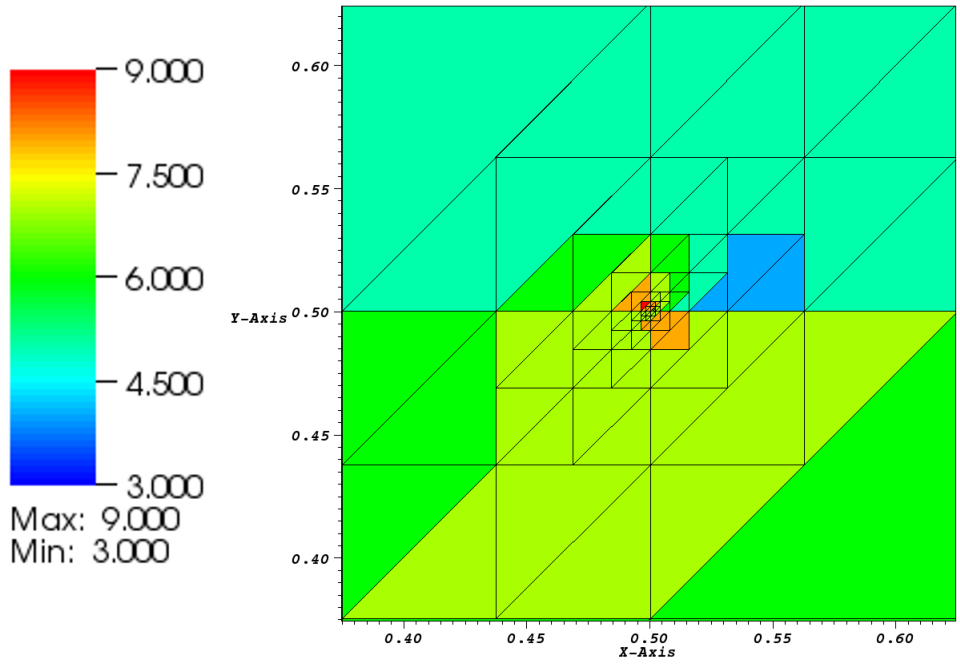

FIGURE 23. Square Domain with Neumann-Neumann Slit: Final mesh and order of polynomials for the second eigenvalue only, showing a close-up of the central portion of the domain (near the singularity).

[10] T. BETCKE AND L. N. TREFETHEN, *Reviving the method of particular solutions*, SIAM Rev., 47 (2005), pp. 469–491 (electronic).

[11] M. BLUMENFELD, *Interface-Eigenwertprobleme auf polaren Gittern*, Z. Angew. Math. Mech., 64 (1984), pp. 266–268.

[12] ———, *The regularity of interface-problems on corner-regions*, in Singularities and constructive methods for their treatment (Oberwolfach, 1983), vol. 1121 of Lecture Notes in Math., Springer, Berlin, 1985, pp. 38–54.

[13] D. BOFFI, *F*inite element approximation of eigenvalue problems, Acta Numer. 19 (2010), 1120.

[14] T. EIBNER AND J. MELENK, *An adaptive strategy for hp-FEM based on testing for analyticity*, Comp. Mech., 39 (2007), pp. 575–595.

[15] S. C. EISENSTAT, *On the rate of convergence of the Bergman-Vekua method for the numerical solution of elliptic boundary value problems*, SIAM J. Numer. Anal., 11 (1974), pp. 654–680.

[16] S. GIANI AND I. G. GRAHAM, *Adaptive finite element methods for computing band gaps in photonic crystals*, Numer. Math., (2011).

[17] S. GIANI, L. GRUBIŠIĆ, AND J. S. OVALL, *Benchmark results for testing adaptive finite element eigenvalue procedures*, Appl. Numer. Math., Volume 62, Issue 2 (2012),pp. 121–140.

[18] L. GRUBIŠIĆ, *On eigenvalue and eigenvector estimates for nonnegative definite operators*, SIAM J. Matrix Anal. Appl., 28 (2006), pp. 1097–1125 (electronic).

[19] L. GRUBIŠIĆ AND K. VESELIĆ, *On weakly formulated Sylvester equations and applications*, Integral Equations Operator Theory, 58 (2007), pp. 175–204.

[20] L. GRUBIŠIĆ AND J. S. OVALL, *On estimators for eigenvalue/eigenvector approximations*, Math. Comp., 78 (2009), pp. 739–770.

[21] P. Houston and E. Süli. A note on the design of hp-adaptive finite element methods for elliptic partial differential equations. *Comp. Methods in Appl. Mech. Eng.*, 194(2-5):229–243, Feb. 2005.

[22] R. B. KELLOGG, *On the Poisson equation with intersecting interfaces*, Applicable Anal., 4 (1974/75), pp. 101–129.

[23] A. KNYAZEV AND O. WIDLUND, *Lavrentiev regularization + Ritz approximation = uniform finite element error estimates for differential equations with rough coefficients*, Math. Comp., 72 (2003), pp. 17–40.

[24] P. D. Ledger, K. Morgan, *T*he application of the *hp*-finite element method to electromagnetic problems, Arch. Comput. Methods Engrg., 12 (2005), pp. 235–302.
[25] B. J. McCartin, *Eigenstructure of the equilateral triangle, part i: The dirichlet problem*, SIAM Review, 45 (2003), pp. pp. 267–287.
[26] J. M. Melenk and B. I. Wohlmuth, *On residual-based a posteriori error estimation in hp-FEM*, Adv. Comput. Math., 15 (2001), pp. 311–331 (2002).
[27] P. Morin, R. H. Nochetto, and K. G. Siebert, *Data oscillation and convergence of adaptive FEM*, SIAM J. Numer. Anal., 38 (2000), pp. 466–488.
[28] S. Sauter, *hp-finite elements for elliptic eigenvalue problems: error estimates which are explicit with respect to λ, h, and p*, SIAM J. Numer. Anal., 48 (2010), 95108.
[29] B. Simon, *Trace ideals and their applications*, vol. 35 of London Mathematical Society Lecture Note Series, Cambridge University Press, Cambridge, 1979.
[30] R. Tankelevich, G. Fairweather, and A. Karageorghis, *Three-dimensional image reconstruction using the PF/MFS technique*, Eng. Anal. Bound. Elem., 33 (2009), pp. 1403–1410.

Durham University, School of Engineering and Computing Sciences, South Road, Durham DH1 3LE, United Kingdom
E-mail address: stefano.giani@durham.ac.uk

University of Zagreb, Department of Mathematics, Bijenička 30, 10000 Zagreb, Croatia
E-mail address: luka.grubisic@math.hr

Portland State University 315 Neuberger Hall Portland, OR 97201, USA
E-mail address: joval l@pdx.edu